Studies on Two Types of Built-in Inhomogeneities for Polymer Gels: Frozen Segmental Concentration Fluctuations and Spatial Distribution of Cross-Links

Tomohisa Norisuye,* Yusuke Kida, Naoki Masui, and Qui Tran-Cong-Miyata

Department of Polymer Science and Engineering, Kyoto Institute of Technology, Matsugasaki, Sakyo-ku, Kyoto 606-8585, Japan

Yasunari Maekawa and Masaru Yoshida

Department of Material Development, Takasaki Radiation Chemistry Establishment, Japan Atomic Energy Research Institute, Watanuki-machi, Takasaki 370-1292, Japan

Mitsuhiro Shibayama

Neutron Scattering Laboratory, Institute for Solid State Physics, The University of Tokyo, Tokai, Naka-gun, Ibaraki 319-1106, Japan

Received January 27, 2003

ABSTRACT: The shrinking kinetics of poly(*N*-isopropylacrylamide) (PNIPA) gels has been studied for two types of PNIPA gels prepared by (i) copolymerization of constituent monomer and cross-linker (monomer cross-linked gels) and (ii) γ-ray irradiation in the PNIPA solutions(polymer cross-linked gels) in order to investigate the role of cross-linking on shrinking kinetics. The shrinking kinetics of the monomer cross-linked gels is quite similar to that of the polymer cross-linked gels. For example, the rapid shrinking is attained by simply lowering the cross-linking density for both types of gels with a skin formation with skin thickness of ca. 3 μm. On the other hand, a significant difference was found when the microscopic structure and the dynamics were investigated by small-angle neutron scattering (SANS) and static/dynamic light scattering (SLS/DLS). The degree of built-in inhomogeneities and dynamic fluctuations were evaluated as a function of the cross-linking degree and the gel preparation temperature by intensity decomposition methods for both types of gels. It is concluded from the SANS and SLS/DLS results that the monomer cross-linked gels have extra built-in inhomogeneities due to the spatial distribution of cross-links in addition to the frozen concentration fluctuations inherent in polymer gels.

Introduction

Hydrogels are three-dimensional network made of polymer chains weakly cross-linked together by covalent bonds and containing a large amount of water.[1,2] They are involved in a diverse range of technologies such as controlled-release systems, super absorbents, size-selective separators, chemo-mechanical device, and so on. The volume phase transition of stimuli-sensitive gels has been fascinating scientists who are trying to understand the fundamental physics of polymer conformation and dynamics for cross-linking system as well as determine various applications. Poly(*N*-isopropylacrylamide) gels are often employed as the model system owing to sensitive conformation change around their transition temperature, $T_c = 34$ °C,[3−7] and the chemical stability at relatively low temperature, $T_c \leq 25$ °C. However it takes more than several hours to days for completion of volume shrinking due to the cooperative nature of gels when the temperature is jumped from room temperature to a temperature above T_c. To overcome such an intricate problem for practical application, rapid-temperature-responsive polymers have designed by various methods, such as (1) introduction of free mobile graft chains into the network,[8] (2) preparation of porous structure with high initial temperature,[9−11] (3) incorporation of mobile linear polymer into network by in situ polymerization in the presence of polymer chains, (4) preparation at low concentration in order to keep the network structure imperfect with long dangling chains,[12,13] and so on. Among a wide variety of molecular and/or structure parameters, structural inhomogeneities are considered as one of the most significant characteristic features governing the physical properties of gels. According to the recent development of microscopic investigations by means of small-angle X-ray(SAXS) or neutron scattering(SANS) and static/dynamic light scattering(SLS/DLS), it is now well-known that network structure in a gel is inherently inhomogeneous due to frozen segmental concentration fluctuations. Hence, the molecular parameters, such as interactions parameters and degree of polymerization between cross-links, should be analyzed properly by taking account of the inhomogeneities and the memory effect of initial condition.

Gels are generally prepared by (i) copolymerizations of monomers and cross-linker (type I) or by (ii) random cross-linking of linear polymer chains via γ-ray radiation or complexation reaction between side functional groups (type II). Type I has often been employed as a familiar procedure with conventional radical polymerization of acrylamide or its derivatives. However, they involve rather complex reaction kinetics originating from the difference of monomer reactivity between monomers and formation of cross-linking clusters due to intrachain cross-linking,[14−16] which leads to formation of additional inhomogeneities with respect to the spatial distribution of cross-links. Therefore, it does not always provide sufficient insight for the network structure and

* To whom correspondence should be addressed.

10.1021/ma030067h CCC: $25.00
Published on Web 07/12/2003

properties of gels. In this study, we discuss the microscopic structure, the dynamics, and the shrinking kinetics of poly(*N*-isopropylacrylamide) gels prepared by the redox copolymerization of monomers (types I) and the γ-ray irradiation of homogeneous polymer solutions (type II) by taking account of two types of built-in inhomogeneities as a function of both the initial temperature and the cross-linking degree.

Experimental Section

Samples. Preparation of γ-ray Gels (Polymer Cross-Linked Gels). Poly(*N*-isopropylacrylamide)(PNIPA) aqueous solutions were prepared by redox polymerization at 20 °C in the presence of *N*,*N*,*N*′,*N*′-tetramethylethylenediamine (TEMED, accelerator) and ammonium persulfate (APS, initiator) in advance to γ-ray irradiation. The monomer solutions were filtered through a 0.2 μm pore size filter before initiating the reaction. Thus obtained polymer solutions were used for the γ-ray irradiation experiment without any further fractionation/purification in order to keep the same condition as the type I system, i.e., the monomer/cross-linker copolymerizing system. Irradiation of γ-ray was carried out by a ^{60}Co source, where the sample was regulated with a thermostat bath at preparation temperatures such as 0, 20, 27, and 30 °C. The γ-ray gels having different cross-linking densities were obtained with different irradiation times ranging from 0.5 to 20 h at constant dose rate of about 10 kGy/h. The γ-ray gels with higher irradiation dose (i.e., 200 kGy) exhibited volume shrinking after irradiation. All the samples were transparent even for the higher irradiation dose. NIPA monomer powder, supplied by Kohjin Chemical Co., was purified by recrystallization prior to use. Reagent grade BIS and APS were purchased from Wakenyaku Co., Ltd., and were used without further purification.

Preparation of Monomer Cross-Linked Gels. A series of PNIPA gels having different cross-linker concentrations were prepared by redox copolymerization and were referred as "monomer cross-linked gel". Monomer solutions were prepared by dissolving monomer and cross-linker, filtered through 0.2 μm pore size filter, as described above. The reaction was initiated by adding TEMED and APS at different preparation temperatures ranging from $T_{prep} = 20-30$ °C. Molar concentrations of BIS, C_{BIS} was varied from 0 to 31.4 mM while that of NIPA, C_{NIPA} was kept to be 690 mM. The details of sample preparation are described elsewhere.[17]

Swelling Degree Measurement. The sample was immersed in a thermostated chamber filled with distilled water. The degree of swelling was measured by monitoring the diameter of the cylindrical gel, *d*, via an inverted microscope (TMD300, Nikon) coupled with an image processor (Algas 2000, Hamamatsu Photonics). The temperature of the chamber was increased either stepwise with $\Delta T \leq 3$ °C by ensuring thermal equilibrium (quasistatic heating) or by temperature jump (*T*-jump) with $\Delta T \geq 20$ °C. The temperature step is defined by $\Delta T = T_{n+1} - T_n$, where T_{n+1} and T_n are the temperatures of the gel at the $(n + 1)$th and nth steps, respectively. In the case of quasistatic heating, *d* was measured after an interval of 30 min whenever the temperature was increased. Then *d* was measured again after another interval of 30 min. If the difference in the values of *d* between two successive measurements was less than 5 μm, temperature was increased again and the same procedure was repeated. By this way, determination of *d* at a quasistatic condition was carried out. On the other hand, *T*-jump was carried out by switching the route of circulating water thermostated at two desired temperatures. The time required for a *T*-jump was about 1 min.

Dynamic Light Scattering. Dynamic light scattering (DLS) measurements were carried out with a DLS/SLS-5000 compact goniometer, ALV, Langen, coupled with an ALV photon correlator. A 22 mW helium−neon laser was used as the incident beam with the wavelength, $\lambda = 632.8$ nm. Time averaged intensity, and the corresponding intensity-correlation function (ICF) were obtained with the acquisition time of 30 s for each run. The intensities and ICFs were collected with various scattering positions by rotating the test cube at fixed scattering angle. The temperature was regulated by thermostat bath within ±0.1 °C.

Small-Angle Neutron Scattering. SANS experiments were carried out on the research reactor, SANS-U, at the Institute for Solid State Physics, The University of Tokyo, located at Japan Atomic Energy Research Institute, Tokai, Japan. A flux of cold neutrons with a wavelength of 0.7 nm was irradiated to the sample, and the scattered intensity profile was collected with an area detector of 128 × 128 pixels. The sample-to-detector distance was set to be 4 m, which covered the accessible *q* range being 0.1−0.78 nm^{-1}, where *q* is the scattering vector. The sample was placed in a brass chamber with quartz windows and the chamber was thermoregulated within an error of ±0.1 °C at the sample position with a NESLAB 110 water circulating bath. The sample thicknesses were in the range 2.20−2.50 mm, depending on the samples. Scattered intensities were circularly averaged by taking account of the detector inhomogeneities, corrected for cell scattering, fast neutrons, transmission, and incoherent scattering, and then scaled to the absolute intensities with a polyethylene standard sample (Lupolen).

Theoretical Background

Dynamic Light Scattering.[18] The time-averaged intensity, $\langle I(t)\rangle_T$ and its correlation functions, $g_T^{(2)}(t)$ defined by

$$g_T^{(2)}(t) \equiv \frac{\langle I(0)I(t)\rangle_T}{\langle I(0)\rangle_T^2} \tag{1}$$

are obtained by a single DLS measurement, where $\langle ...\rangle_T$ denotes a time average. For an ergodic system, they are considered to be equivalent with an ensemble average correlation function, $g_E^{(2)}(t)$, that is

$$g_T^{(2)}(t) = g_E^{(2)}(t) \equiv \frac{\langle I(0)I(t)\rangle_E}{\langle I(0)\rangle_E^2} \tag{2}$$

where $\langle ...\rangle_E$ denotes an ensemble average. For colloidal glasses and gels, however, the time-averaged properties differ from the sample-averaged properties due to localization of chain segments with cross-links even if the intensity was averaged over an enough duration time. It is called "restricted ergodicity" or "nonergodicity". The former may be relevant to represent the present system since the equilibrium state for gels is uniquely determined when the full ensemble is obtained by collecting the scattered intensity over the entire space. From this aspect, gels differ from a nonergodic system, which has many energy minima depending on the way of approaching its equilibrium state. Such a restricted nature for gels is often observed as the spikelike intensity fluctuations with sample position, called speckles,[19−23] when the intensity is observed by scanning sample position. Here, the observed intensities include uninteresting heterodyne component generated by illumination of immobile segments acting as a local oscillator and/or by stray lights. Therefore, the pure homodyne component should be extracted by extrapolating the scattered intensity to the low intensity limit. Since only local motion between cross-links with small amplitude is allowed for the system, the intensities, i.e., the squares of the scattering field for noninteresting strong heterodyne component are often observed as a superposition of fluctuations. That is, the observed

intensity $I(t)$ may be written by

$$I(t) = I_F(t) + I_C \tag{3}$$

where $I_F(t)$ and I_C are the intensity components for time-dependent thermal fluctuations and time-independent frozen inhomogeneties, respectively. By replica field approach, Panyukov and Rabin theoretically derived the above superposition rule without any assumption. The same rule is applied in analysis of dynamic light scattering. For example, according to Pusey[18] et al. and Geissler,[24] showed that $g_T^{(2)}(t)$ for the restricted system can be expressed by

$$g_T^{(2)}(t) = 1 + X^2 g_F^{(1)}(t)^2 + 2X(1 - X)g_F^{(1)}(t) \tag{4}$$

where X and $g_F^{(1)}(t)$ are the ratio of intensity for the thermal fluctuations to the total intensity and the fully fluctuating component of the field correlation function, respectively. That is

$$X \equiv \frac{\langle I_F \rangle_T}{\langle I \rangle_T} \tag{5}$$

$$g_F^{(1)}(t) = \frac{\langle E_F(0)E_F^*(t)\rangle_E}{\langle I_F(0)\rangle_E} = \frac{\langle E_F(0)E_F^*(t)\rangle_T}{\langle I_F(0)\rangle_T} \tag{6}$$

Note that the initial amplitude of the time−intensity correlation function

$$\sigma_I{}^2 \equiv g_T^{(2)}(0) - 1 = \frac{\langle I(0)^2\rangle_T}{\langle I(0)\rangle_T{}^2} \tag{7}$$

is less than unity for restricted-ergodic systems due to existence of strong frozen component. As can be found in the collective diffusion theory, $g_F^{(1)}(t)$ can be approximated with short time expansion as follows,

$$g_F^{(1)}(t) \cong 1 - Dq^2t + ... \tag{8}$$

After trivial mathematical treatment, $g_T^{(2)}(t)$ can also be expressed as the following

$$g_T^{(2)}(t) = 1 + \sigma_I{}^2(1 - D_A q^2 t + ...) \tag{9}$$

where

$$D_A = \frac{D}{2 - X} \tag{10}$$

is the apparent diffusion coefficient from single measurement. Substituting zero into eq 2, we will arrive at

$$\sigma_I{}^2 = X(2 - X) \tag{11}$$

This is called the "heterodyne" or "partial heterodyne" approach. With some arrangements we arrive at[17,25]

$$\sigma_I{}^2\langle I\rangle_T{}^2 = 2\langle I_F\rangle_T\langle I\rangle_T - \langle I_F\rangle^2 \tag{12}$$

or

$$\frac{\langle I\rangle_T}{D_A} = \frac{2}{D}\langle I\rangle_T - \frac{\langle I_F\rangle_T}{D} \tag{13}$$

The plot of the lhs with $\langle I\rangle_T$ gives $\langle I_F\rangle_T$ and D from the intercept and slope, respectively.

Panyukov−Rabin Theory for SANS Analysis.[26,27] According to the PR theory, the scattering intensity, $I(q)$, can be decomposed to two fluctuating components of the structure factor, $S(q)$, i.e., the dynamic correlator, $G(q)$, and the static correlator, $C(q)$. The former represents the thermal fluctuations of the reference polymer solution, while the latter is related to the built-in inhomogeneities introduced by cross-linking. Hence, the total scattering intensity is written by

$$I(q) = KS(q) = K[G(q) + C(q)] \tag{14}$$

where K is the scattering vector and the proportional constant.

The thermal correlator, $G(q)$, can be written by

$$G(q) = \frac{\phi N g(q)}{1 + wg(q)} \quad \text{(for gels)} \tag{15}$$

or

$$G(q) = \frac{\phi N}{\frac{Q^2}{2} + w} \quad \text{(for solutions)} \tag{16}$$

where

$$g(q) = \frac{1}{Q^2/2 + (4Q^2)^{-1} + 1} + \frac{2}{(1 + Q^2)^2(\phi_0/\phi)^{2/3}} \tag{17}$$

is the thermal correlator in the absence of the excluded volume effect and

$$w = (1 - 2\chi + \phi)\phi N \tag{18}$$

is the excluded volume parameter. ϕ and ϕ_0 are the volume fraction of the gel at sample preparation and at observation, respectively. N is the average degree of polymerization between cross-links. Q is the reduced scattering vector normalized by the monomer fluctuating radius. The static correlator, which corresponds to the contribution from the frozen structure of gels, is given by

$$C(q) = \frac{\phi N}{[1 + wg(q)]^2(1 + Q^2)^2}\left[6 + \frac{9}{w_0 - 1 + (^1/_2)Q^2\left(\frac{\phi_0}{\phi}\right)^{2/3}}\right] \tag{19}$$

where w_0 is the excluded volume parameter at sample preparation

$$w_0 = (1 - 2\chi_0 + \phi_0)\phi_0 N \tag{20}$$

Alternatively, w_0 can be expressed by

$$w_0 = \phi_0{}^{5/4} N \tag{21}$$

depending on the state at preparation.

Results and Discussion

Figure 1 shows the time course of swelling ratio, d/d_0, for (a) the PNIPA monomer cross-linked gels and (b)

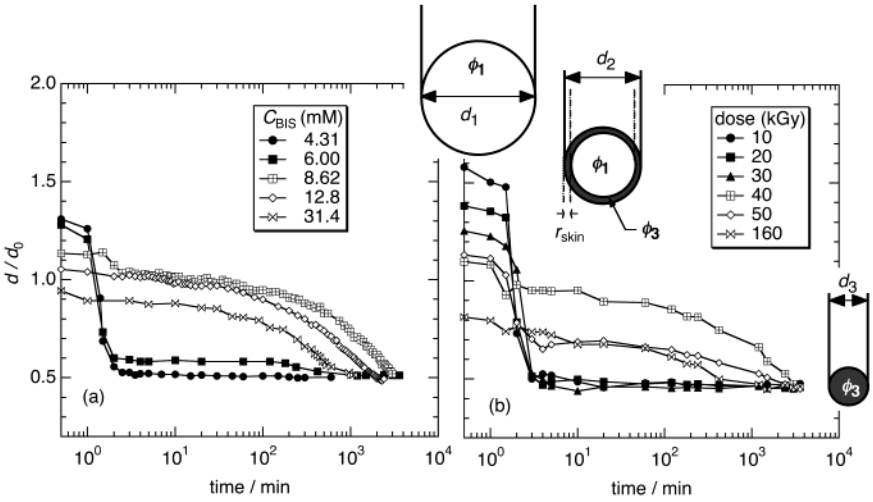

Figure 1. Time course of swelling ratio, d/d_0, for (a) the PNIPA monomer cross-linked gels and (b) the γ-ray cross-linked gels with different cross-linking concentrations, after T-jump from 20 to 45 °C, where d and d_0 are the diameters of the gel at observation and preparation, respectively. The insets schematically show the cross section of cylindrical gels with the definition of the diameters, the volume fraction, and the skin thickness, before and after T-jump.

the γ-ray cross-linked gels with different cross-linking concentrations, after a T-jump from 20 to 45 °C, where d is the diameter of the gel at observation and d_0 is the capillary diameter at which the gel was formed. As can be seen from the figure, rapid shrinking was attained by simply lowering the cross-linker concentration or the irradiation dose for both types of gels indicated by filled symbols. A similar result is reported earlier for the monomer cross-linked gels. An abrupt change from rapid to slow shrinking was found around $C_{BIS} = 8.62$ mM for the monomer cross-linked gels and around irradiation dose of 40 kGy for the γ-ray irradiated gels. Two-step shrinking was also observed for both gels at the critical cross-linking density for the rapid shrinking, i.e., 8.62 mM and 40 kGy. Although the unit of cross-linking degree was different in the two types of gels, we obtained the following relation from the critical densities in this study as

$$[\text{irradiation dose (kGy)}] = 4.64[C_{BIS}\,(\text{mM})] \quad (22)$$

for the PNIPA gels with $T_{prep} = 20$ °C. There are two possibilities to exhibit such a two-step reduction of the swelling ratio. One is formation of the skin layer and the other is a two-step shrinking via crumpled globule formation proposed by Grosberg[28] and by Dowson et al.,[29,30] i.e., chain shrinking and subsequent intracluster association. Let us first discuss the first possibility in more detail.

When a gel is immersed in hot water, the temperature of the gel increases above the transition temperature, resulting in phase separation followed by gel shrinking. However, shrinking can take place only at the surface and the inner part of gels is not allowed shrinking because outgoing water is blocked by surface shrinking, i.e., skin formation. Therefore, the skin formation plays a major role in slow shrinking as discussed in the literature.[8] If the skin layer is formed in the first step, the concentration for the condensed surface will be the same as that for the complete shrunken state. Thus, the following mass conservation equation can be assumed for cylindrical gels before and after shrinking provided that (1) the inner part of the gel remain in the swollen state and (2) the length of the gel is unchanged,

$$\phi_{swollen} S_{swollen} = \phi_{shrunken} S_{skin} + \phi_{swollen} S_{internal} \quad (23)$$

where ϕ and S are the volume fraction and the cross section, respectively. When a gel is immersed in hot water, the gel shrinks from the swollen state (state 1) to the intermediate state (state 2), followed by complete shrinking (state 3). Hence, eq 23 is written by

$$\phi_1 \pi \left(\frac{d_1}{2}\right)^2 = \phi_3 \pi \left[\left(\frac{d_2}{2}\right)^2 - \left(\frac{d_2}{2} - r_{skin}\right)^2\right] + \phi_1 \pi \left(\frac{d_2}{2} - r_{skin}\right)^2 \quad (24)$$

where d_i ($i = 1, 2, 3$) and r_{skin} indicate the diameters and the thickness of the skin layer and the number in subscript denote the state defined above. Since the volume fraction is proportional to the reciprocal cubic power of the linear swelling ratio, one obtains

$$\phi_i \approx \phi_0 \left(\frac{d_0}{d_i}\right)^3 \quad (25)$$

where $i = 1, 2, 3$. By substituting eq 25 into eq 24, we get,

$$r_{skin} = \frac{d_0}{2}\left(d_2 - \sqrt{\frac{d_3^{\,3}\, d_1^{\,2} - d_1^{\,3}\, d_2^{\,2}}{d_3^{\,3} - d_1^{\,3}}}\right) \quad (26)$$

In our case, r_{skin}s for the monomer cross-linking and polymer cross-linking systems were evaluated as 2.50 and 3.44 μm, respectively. The second possibility is that the initial chain shrinking and subsequent intracluster association. However, the second possibility, i.e., the two-step shrinking via crumpled globule formation, does not seem to be adequate for the rapid shrinking because it requires macroscopically homogeneous shrinking as is the case of dilute polymer solutions. Therefore, we expect that above skin-layer formation is the reason for two-step shrinking and skin layer formation is one of major criteria for slow shrinking kinetics. Despite the different cross-linking methods, both gels exhibit a similar shrinking kinetics.

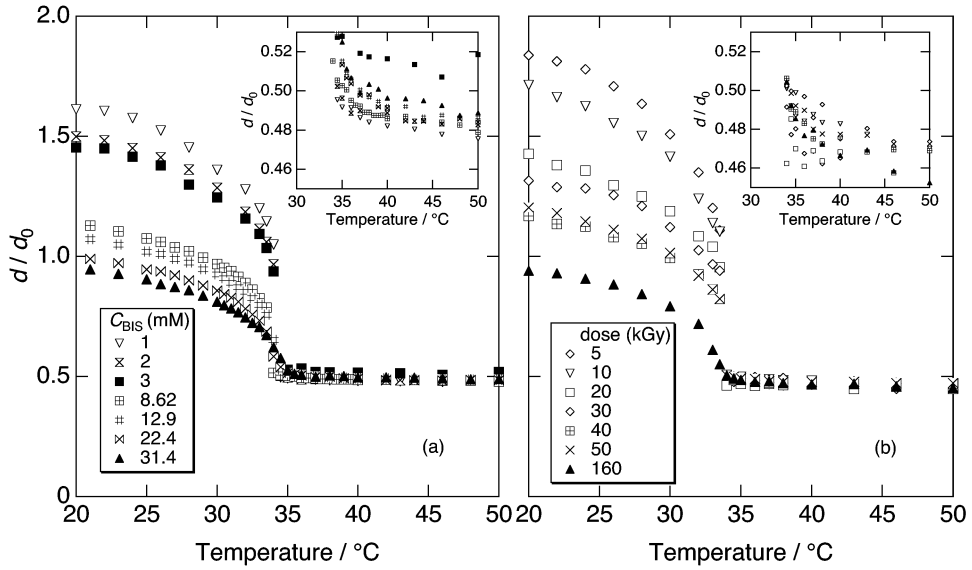

Figure 2. Equilibrium swelling curves for (a) the monomer cross-linked gels and (b) the polymer cross-linked gels with different cross-linking concentrations. To demonstrate the difference of compactness just above transition temperature for both gels, the transition regions of the swelling curves are shown in the insets.

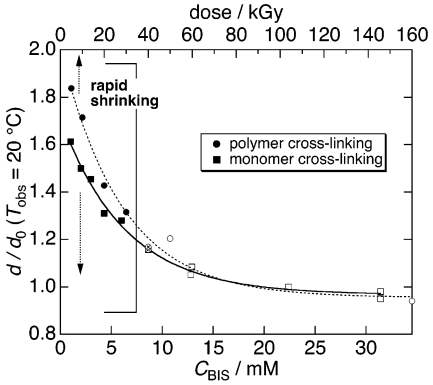

Figure 3. d/d_0s at the observation temperature $T_{obs} = 20$ °C plotted with C_{BIS} for the monomer cross-linked gels in the bottom axis and with the irradiation dose for the γ-ray gels in the top axis.

Figure 2 shows equilibrium swelling curves for (a) the monomer cross-linked gels and (b) the polymer cross-linked gels with different cross-linking concentrations. To demonstrate the difference of compactness just above the transition temperature for both gels, the transition regions of the swelling curves are shown in the insets. For both gels, volume phase transition occurs around 34 °C and the shrinking process systematically changes from discontinuous to continuous transitions with increasing cross-linking degree. However, as shown in the inset of the figure, the values of d/d_0 for the monomer cross-linked gels are higher than that for the γ-ray cross-linked gels. The difference appeared in the shrunken state may result from the difference in spatial structure. In our previous work,[31] we made a comparison of structure factors for the monomer cross-linked gels and the γ-ray cross-linked gels by means of small-angle neutron scattering with Panyukov−Rabin theory. For both gels, segmental concentration becomes frozen at the onset of gelation, resulting in gels being inherently inhomogeneous. However, the monomer cross-linked gels include the difference of the monomer-reactivity ratio and the formation of inter-cross-linking clusters, suggesting a higher degree of imhomogeneities.

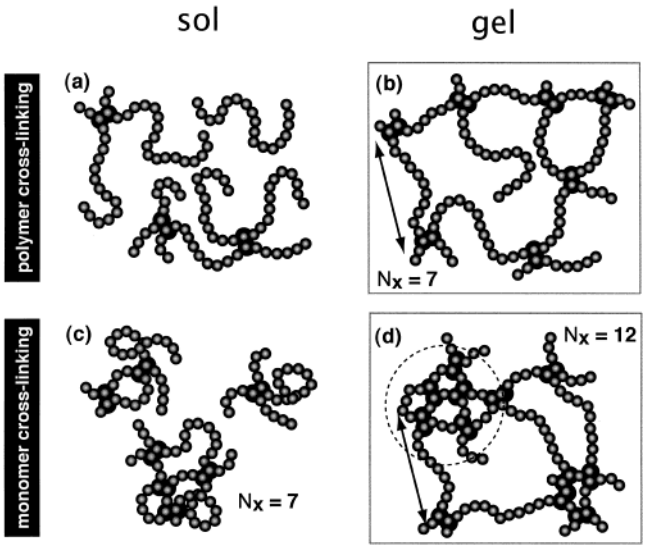

Figure 4. Schematic models for the polymer cross-linking system (a and b) and for the monomer cross-linking system (c and d). N_x is the number of cross-links in the figure.

Such a difference concerning the spatial structure is clearly recognized when d/d_0 at equilibrium swelling is plotted with respect to the cross-linking degree. In Figure 3, d/d_0 at 20 °C is plotted with C_{BIS} for the monomer cross-linked gels in the bottom axis and with the irradiation dose for the γ-ray gels in the top axis. The vertical solid line indicates the concentration at which the following two criteria meet: (1) rapid to slow shrinking boundary and (2) the point where the two-step shrinking was found. The conversion of the cross-linking degree for two types of gels was proposed above (see eq 22). Also, the validity of the conversion will be examined by cross-linking density dependence of the homodyne diffusion coefficient in the subsequent section. As can be seen from the figure, clear difference for d/d_0 is found in the lower cross-linking region, e.g., $C_{BIS} < 15$ mM.

From the above experimental findings, we propose a schematic model for the polymer cross-linking system in Figure 4,parts a and b and for the monomer cross-

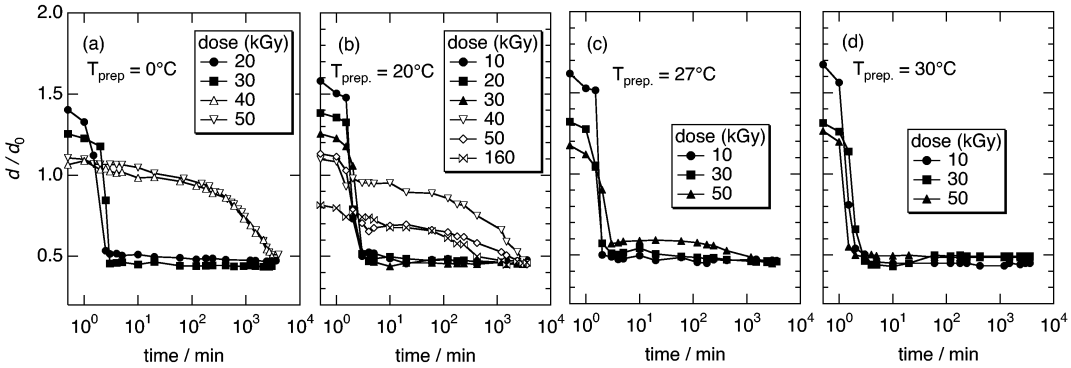

Figure 5. Time course of d/d_0 for gels undergoing shrinking transition after T-jump from 20 to 45 °C. These gels have different cross-linking degrees for the γ-ray gels and are prepared at (a) 0, (b) 20, (c) 27, and (d) 30 °C.

linking system in Figure 4, parts c and d. For the polymer cross-liking system, chains are loosely connected together but remain in the sol state at a low cross-linking degree (Figure 4a). With increasing irradiation dose, a γ-ray gel having random distribution of cross-links is formed as shown in Figure 4b. On the other hand, a larger amount of cross-links is required to form a gel for the monomer cross-linking system due to the penalty of cross-linking formation by intra-cross-linking and/or difference of monomer reactivity ratio between monomer and cross-linker. Thus, as shown in Figure 4c, a gel cannot be formed with the same number of cross-links, e.g., $N_X = 7$, as in part b as indicated by the number of cross-links, N_X. When further cross-links ($N_X = 12$) are introduced (part d), the clusters are interconnected together, resulting in infinite network formation. The monomer cross-linking gels have almost the same distance between cross-links as indicated by arrows, but the cross-linker rich domains are incorporated in the structure, resulting in higher average cross-linking density. This may lead to the difference of d/d_0 at relatively low cross-linking degree in Figure 3. Further introduction of cross-links results in a similar dense structure for both types of gels.

One of the most important features to understand gels is the fact that gels memorize the state of their preparation. The chain conformation of PNIPA in aqueous solutions gradually varies from an expanded to collapsed states at low and high temperatures, respectively, since the solutions exhibit an LCST phase diagram. Needless to say, the higher the preparation temperature, the more inhomogeneous the resultant gel is. When we introduce cross-linker into the system, cross-link is formed at the binary contacting points between chains. Therefore, the number of cross-links incorporating network formation depends on the polymer−polymer interaction at the initial condition. This means that the higher the preparation temperature, the easier the chain connection similar to the chain association. In other words, a limit, called the cross-linking saturation threshold (CST), is easily attained for the higher preparation temperature.[31,32] To clarify this point, we investigated the preparation temperature dependence of shrinking kinetics. Figure 5 shows the time course of d/d_0 for gels after T-jump from 20 to 45 °C. These gels had different cross-linking degrees for the γ-ray gels prepared at (a) 0, (b) 20, (c) 27, and (d) 30 °C. As described above, the γ-ray gels prepared at relatively low temperatures with low cross-linking densities exhibited rapid shrinking. With increasing preparation temperature, T_{prep}, rapid shrinking was observed for all

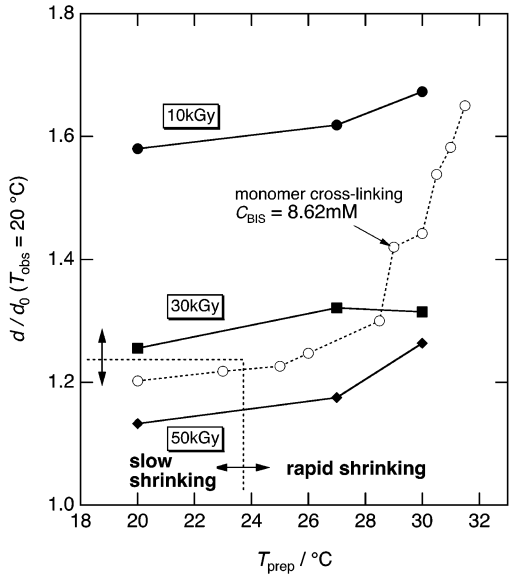

Figure 6. d/d_0 (at 20 °C) vs T_{prep} for the γ-ray gels (filled symbols) and for the monomer cross-linked gels (open symbol).

of the samples having different cross-liking densities. A similar phenomenon was observed for PNIPA gels prepared by monomer copolymerization. Hence, this seems to be a universal feature irrespective of the method of cross-linking.

A striking difference in the cross-link degree dependence of d/d_0 between the monomer cross-linking gels and the γ-ray gels was observed when d/d_0 at fully swollen state was plotted with T_{prep}. As shown in Figure 6, d/d_0 increased with T_{prep} for the γ-ray gels (filled symbols), indicating the formation of loose network. This result is consistent with that in the previous report[33] for the monomer cross-linking system (open symbols). However, the T_{prep} dependence seems to be rather weak for the γ-ray gels compared to that of the monomer cross-linked gels. The values of d/d_0s for the monomer cross-linked gels with low T_{prep}s are located between the values for the γ-ray gels with irradiation dose of 30 and 50 kGy. The d/d_0 for the monomer cross-linking system, however, drastically increased with T_{prep} and finally reached the values nearly equal to that for the γ-ray gels with the irradiation dose of 10 kGy. This may indicate that significantly loose and ineffective cross-linking formation occurs for the monomer cross-linked gels due to congregation of cross-linkers. The reactivity of monomers and/or radical activity of initiator may also cause such a behavior. A rapid shrinking is attained for

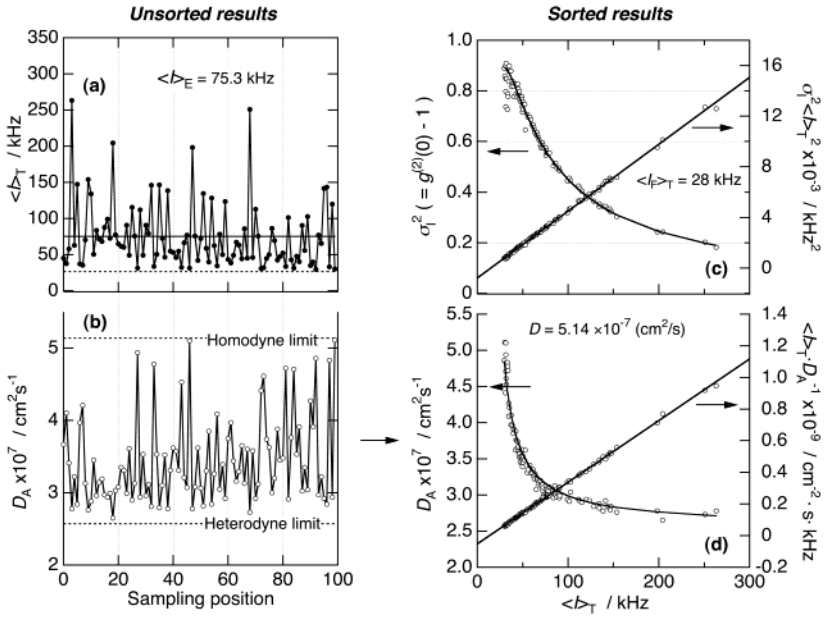

Figure 7. Typical examples of the DLS data analysis: (a) time-averaged scattered intensities, $\langle I \rangle_T$, and (b) the corresponding apparent diffusion coefficients, D_A, measured at various sample positions. The strong fluctuation with the sample position, called speckle, was often observed for gelling system. Since a strong scattering is an uninteresting component, $\langle I \rangle_T$ and D_A were sorted with the intensities and the dynamic component of the intensity and the diffusion coefficient were evaluated as described in the context (c and d).

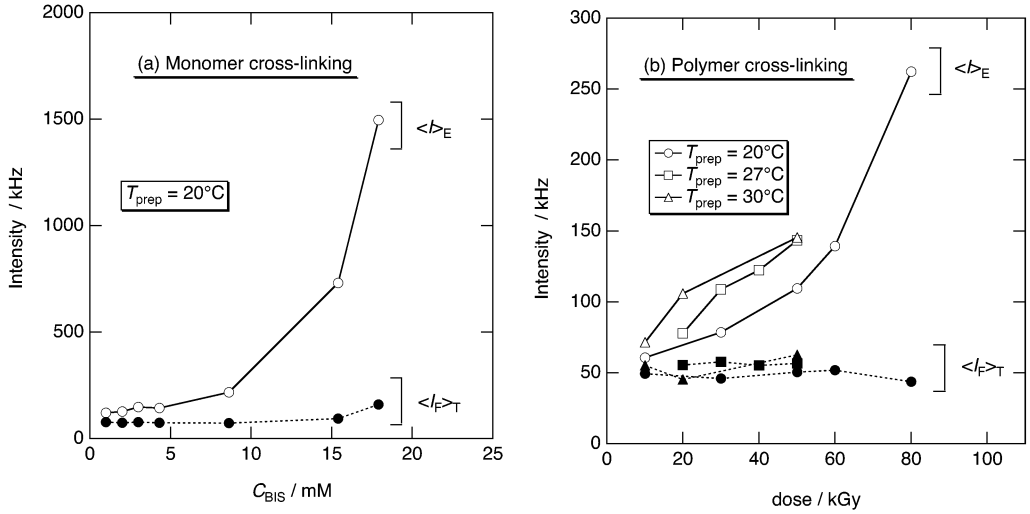

Figure 8. Ensemble averaged intensity $\langle I \rangle_E$ and the thermal contribution $\langle I_F \rangle_T$ as a function of cross-linking degree for (a) the monomer cross-linked gels and (b) the polymer cross-linked gels. The intensities for the polymer cross-linking system with different T_{prep}s were also demonstrated in Figure 8b.

T_{prep} above 24 °C or d/d_0 above 1.25 as indicated in the figure.

To investigate the structure and the dynamics for both types of gels, dynamic light scattering experiments have been conducted by deeply taking account of the inhomogeneities. In Figure 7, typical examples of the data analysis were shown. The time-averaged intensity, $\langle I \rangle_T$, and the apparent diffusion coefficient, D_A, were obtained at many sample positions by rotating the test tube and were plotted with the sample position in Figure 7, parts a and b, respectively. Since the spikelike intensity pulses are uninteresting data in case the pure homodyne diffusion being explored, D_A and the initial amplitude of the intensity correlation function, σ_I^2, are sorted as a function of the intensity according to the following methods. First, $\langle I \rangle_T$, was decomposed into two components, namely, the thermal fluctuations $\langle I_F \rangle_T$ and the frozen inhomogeneities $\langle I_C \rangle_E$ by curve fitting with eq 11 as shown in Figure 7c. Alternatively, the same results were obtained by a linearized fit with eq 12. Then, the collective diffusion coefficient, D, corresponding to the pure homodyne mode was evaluated by fitting with eq 10 or the linearized function of eq 13 while fixing the value of $\langle I_F \rangle_T$ obtained above. By this method, $\langle I_F \rangle_T$, $\langle I_C \rangle_E$, and D for all the gels were evaluated.

The ensemble averaged intensity $\langle I \rangle_E$ and the thermal contribution $\langle I_F \rangle_T$ were shown for the monomer cross-linked gels and the polymer cross-linked gels in Figure 8, parts a and b, respectively. The intensities for the polymer cross-linking system with different T_{prep}s were also demonstrated in Figure 8b. It is well-known that the test tube for the γ-ray irradiated sample was colored brown after γ-ray irradiation. Therefore, a correction for the transmission was carried out by measuring the intensity of standard toluene in discolored test tube normalized by that in the clear one without irradiation.

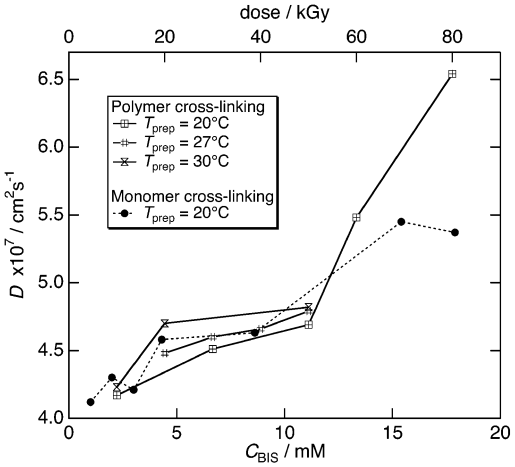

Figure 9. Homodyne diffusion coefficient, D as a function of the cross-linking density for both types of gels. D for the polymer cross-linking system with different T_{prep}s was also presented.

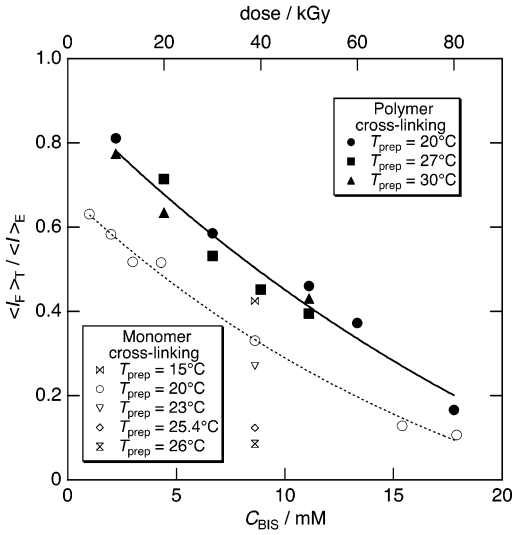

Figure 10. Variation of $\langle I_F \rangle_T / \langle I \rangle_E$'s as a function of cross-liking density for the monomer cross-linked gels (open symbols) and the γ-ray gels (filled symbols). The solid and dotted lines are drawn for the eye.

The transmissions measured with 10, 30 and 50 kGy were 0.89, 0.83 and 0.79, respectively. Therefore, the following empirical equation is obtained:

$$[\text{transmission}] = 0.79 + 0.21 \times \exp(-0.065[\text{dose}]) \quad (27)$$

$\langle I \rangle_E$ increased with cross-linking density for both gels, while the contributions of the thermal fluctuations are rather weak and independent of the cross-linking density. It is concluded that the increase of the ensemble-averaged intensity is due to frozen inhomogeneities. However, the inhomogeneities for the monomer cross-linking system are much larger than that of the polymer cross-linking system, suggesting that an extra contribution for inhomogeneities exists for the monomer cross-linking gels, such as cross-linking cluster formation. $\langle I_F \rangle_T$s for the polymer cross-linking gels with different T_{prep} are rather constant as reported in the earlier paper,[34,35] and $\langle I_F \rangle_T$ is only dominated by observation conditions.

To evaluate the true dynamics, D_As are extrapolated to pure homodyne limit with eq 10 or eq 13. Extracted D as a function of the cross-linking density for both types of gels together with different T_{prep}s are shown in Figure 9. Note that the D increases with increasing cross-linking density for two types gels irrespective of the way of cross-linking. Although the two types of gels are described with different units of cross-linking density as mentioned above, D for the two types of gels falls on a single master curve and linearly increases with increasing cross-link degree. The increase of D with increasing cross-link degree is reasonable since the inverse of D is proportional to the mesh size which is decreasing with the cross-link degree, i.e., $D \sim \xi^{-1}$.[36] Surprisingly, D is independent of T_{prep}. This fact indicates that the dynamic properties such as D are not dependent on T_{prep} but on the observation temperature, T_{obs}.

As an indicator of the degree of homogeneity, the variation of $\langle I_F \rangle_T / \langle I \rangle_E$'s for both types of gels is shown in Figure 10 as a function of cross-linking density. For all the T_{prep}s, $\langle I_F \rangle_T$ for the polymer cross-linked gels are larger than that for the monomer cross-linking gels, indicating that the polymer cross-linked gels are less inhomogeneous. The T_{prep} dependence is also weak for the polymer cross-linking system (solid symbols) which is opposite to the case of the monomer cross-linking system (open symbols).

To elucidate the origin of frozen inhomogeneities, small-angle neutron-scattering experiments have been conducted for both types of gels. The scattering functions for the γ-ray gels having different irradiation doses prepared at (a) 0, (b) 20, (c) 27, and (d) 30 °C were shown as a function of the wave vector in Figure 11. For all the preparation temperatures, the scattering intensity, $I(q)$, for the PNIPA solutions indicated by open circles is described by a Lorentz function. On the other hand, those for gels deviate from Lorentz behavior at the low q region. The intensity increased with the irradiation dose, indicating the larger contribution from frozen inhomogeneities.[37,38] A series of the γ-ray gels prepared at 0 °C are rather homogeneous. This is because cross-links are introduced at a temperature far below LCST. Contrary to the low q behavior, $I(q)$s marge at high q region irrespective of the irradiation dose except that for 200 kGy. It should be noted the following. Since noticeable syneresis, i.e., volume shrinking, was observed for irradiation dose of 200 kGy after irradiation of γ-ray, the intensity was normalized by the volume fraction evaluated by equilibrium swelling measurements as shown in Figure 11a.

As reported in our previous paper, the scattering function for PNIPA gels can be well described by the Panyukov−Rabin theory, which takes into account both condition at observation and the preparation. The solid lines indicated in the figures are the results of fitting by the PR theory with eqs 14−20 where the known values, such as the segment length, $a = 8.12$Å,[39,40] and the volume fraction, $\phi = 0.078$, are employed as fixed parameters. As demonstrated in our previous paper, we first determined independently the interaction parameters at the observation and preparation condition, χ and χ_0, respectively. χ is evaluated by fitting the solution data to eq 16 without additional adjustable parameter whereas the values of χ_0 for 20, 27, and 30 °C being 0.39, 0.45, and 0.48, respectively, are taken from our previous paper.[32] All the following analyses have been carried out by fixing the known parameters, a, ϕ, χ, and χ_0. Thus, the fitting parameter is only the degree of

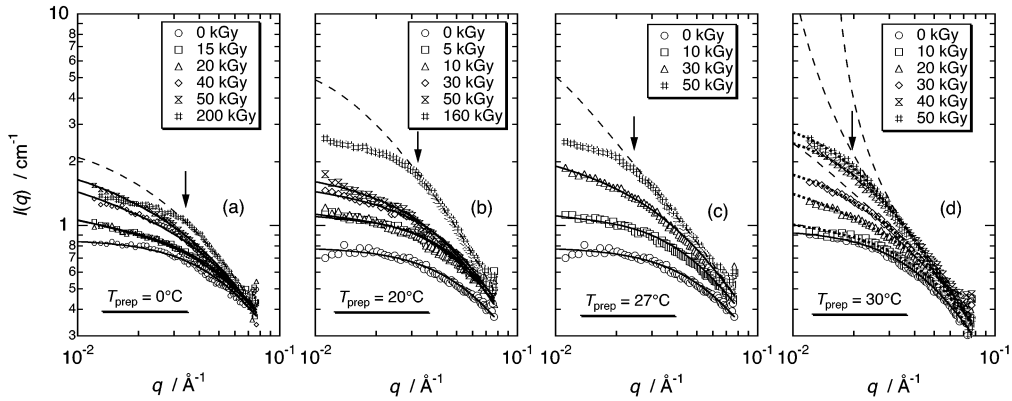

Figure 11. Neutron scattering intensity functions for the γ-ray gels prepared with different irradiation doses and at (a) 0, (b) 20, (c) 27, and (d) 30 °C. The experimental curves level off at a wave vector, indicated by solid arrows. The correlation length, proportional to the inverse of the q value at the arrow position, seems to shift to lower q with increasing T_{prep}. The scattering functions are well reproduced by the theory except for the case of high irradiation doses (dashed lines). The PR theory completely fails to reproduce the experimental data for $T_{prep} = 30$ °C with a single set of parameters. Alternatively, the theoretical functions calculated by the scaling approach are represented by dotted line in part d.

polymerization between cross-links, N, and the contrast factor, K.

For the γ-ray gels with $T_{prep} = 0$ °C, the scaling approach, eq 21, was applied instead of eq 20. That is true as far as the sample is prepared at a limit of good solvent condition, e.g., sufficiently far from the critical solution temperature. On the other hand, the mean field approach was applied for the γ-ray gels prepared above 20 °C. The validity of the two approaches, i.e., the scaling and the mean-field approach, are discussed in the previous paper based on the calculation of crossover point with two approaches.[31] The curve fitting seems to be successful for all the irradiation doses except that for the highest irradiation dose of 200 kGy where the PR theory significantly overestimated the intensity at the low q. The breakdown of the PR theory may be ascribed to the fact that the theory assumes instantaneous cross-linking and no structural relaxation is considered during cross-linking formation. Moreover, the excess irradiation may lead to rather homogeneous structure filled with a dense mesh. Note that chain scission is not taken into account here, which may be additional effect to make such results. Thus, the scattering function with the highest irradiation dose failed to be represented by the PR theory, which predicts a power-law like scattering function[25,38,41−43] and occurrence of divergence of the intensity at low q for the highest irradiation dose.

Although the scattering function deviates from the theoretical curve, the experimental curves level off at a wave vector, indicated by a solid arrow. The correlation length, proportional to the inverse of the q value at the arrow position, seems to shift to lower q with increasing T_{prep}. This means, in a sense, the structure of the γ-ray gels become inhomogeneous with increasing T_{prep}.

Subsequently, the fitting analyses have been conducted for a series of the γ-ray gels with various T_{prep}. As shown in Figure 11b the scattering functions are well reproduced by the theory except for the case of 160 kGy. For Figure 11c, the fitting becomes poor even in a typical irradiation dose, e.g., 50 kGy. The functions seem to be similar but the possible number of cross-links capable of incorporation into network is considered to be different. It should be noted that the scattering functions for a series of γ-ray gels exhibit completely different phenomena compared to those for the monomer cross-linked gels as shown in our previous paper.[31] A power-law behavior or an upturn of the scattering intensity for lower q observed in our previous study has not been observed yet, although the shape of the functions becomes similar to that for the monomer cross-linked gels for $T_{prep} = 27$ or 30 °C. Instead of the low q upturn of the intensity as indicated by dash line in Figure 11c, the gel becomes a shrinking gel while keeping the transparency. Therefore, on the contrary to the monomer cross-linked gels, the power-law-like behavior and divergence of the intensity at low q limit will be never attained even if further γ-ray irradiation is performed.

As shown by the dashed line in Figure 11d, the PR theory completely fails to reproduce the experimental data for $T_{prep} = 30$ °C with a single set of parameters. Alternatively, the theoretical functions calculated by the scaling approach are represented by dotted line in the figure in order to demonstrate the role of inhomogeneity in the PR theory. The dotted lines with scaling approach fit better rather than the dashed lines for the mean filed approach with $\chi_0 = 0.48$. This means, conversely, that the PR theory overestimates the contribution of frozen inhomogeneities in the process of deriving the static correlator, $C(q)$. Originally, the PR theory was proposed in order to represent the scattering behavior for a gel instantaneously cross-linked with long chains in SANS region. This assumption is expected to well describe γ-ray gels rather than monomer cross-linked gels. However, curiously enough, the latter system succeeded in reproducing the theoretical scattering behavior (although not supported in the theory), while the former is partially applicable but not completed. Since the PR theory addresses the importance of frozen inhomogeneities for polymer gels and includes important parameters such as interaction parameters and degree of cross-links, the structure factor predicted by this theory is much better than the phenomenological functions such as Gauss, Lorentz, or Debye−Bueche functions. However, the improvement of the theory, in particular the calculation of degree inhomogeneities, with reconsideration of two types of built-in inhomogeneties, i.e., the contributions originated from (1) the frozen concentration fluctuations and (2) monomer reaction or formation of cross-linking clusters, would be necessary. The former is inherent in the cross-linking system, whereas the latter is introduced when a gel is formed from monomers with chemical reaction.

Conclusions

The rapid and slow shrinking kinetics for temperature sensitive gels have been investigated by the swelling ratio measurement as a function of the cross-linking density and the preparation temperature. The conventional monomer cross-linking and the γ-ray irradiation methods were employed in order to explore the role of cross-linking on the swelling/deswelling kinetics. The rapid shrinking was achieved when a gel was formed at low cross-linking density and/or prepared at high-temperature irrespective of the way of cross-linking. Here, a two-step shrinking takes place with skin formation of which the thickness is ca. 3 μm for both types of gels. However, a significant difference of the linear swelling ratios was found at the fully swollen state. The difference was discussed based on the mechanism of cross-linking formation and its efficiency. For the monomer cross-linking system, larger amount of cross-links are required to form a gel due to the cross-linker-rich domain formation. On the other hand, the γ-ray gels exhibited rather homogeneous structures compared to that of the monomer cross-linking system. Note that built-in inhomogeneities still exist in the γ-ray gels due to frozen concentration fluctuations.

The difference in two types of inhomogeneities appears when the light or neutron scattering intensity for static contribution was compared between the two types of gels as a function of cross-linking density. Because of the difference of monomer reactivity ratios and formation of microgel clusters, the monomer cross-linking gels exhibited extraordinarily strong scattering behavior. Although this phenomenon is more or less related to frozen inhomogeneties in the gelling system, one should be aware that they include different physical meanings with the inhomogeneous structure inherent in cross-linking system.

Apart from the static inhomogeneities, the dynamic parts, such as $\langle I_F \rangle_T$ and D are independent of the method of cross-linking. $\langle I_F \rangle_T$ depends only on the observation conditions, such as observation temperature or polymer concentration, and thus it is an invariant with respect to the initial condition. If the thermal fluctuations and the frozen inhomogeneities are properly decomposed into each contribution, the homodyne diffusion coefficient, D, is extracted from apparent values obtained by sample rotation. An increase of D (decrease of ξ) with the cross-linking density was found for the γ-ray gels as well as the monomer cross-linked gels, indicating the cross-linking is certainly introduced into the network with γ-ray irradiation or cross-linker concentration.

The PR theory allowed us to make a concrete discussion about inhomogeneous network structure and to reproduce our experimental results for the SANS functions of the PNIPA gels prepared by conventional radial polymerization of monomers as reported before. However, the theory was not applicable for the γ-ray gels when the gel was prepared at higher irradiation dose or even high preparation temperature. In addition, the scaling approach ensures the suppression of apparent inhomogeneities by strong thermal fluctuations and instead succeeded in reproduction of our data. The theory was originally proposed in order to describe the scattering behavior of gels cross-linked with long polymer chain. Nevertheless, the theory fails to reproduce the scattering functions for polymer cross-linking system and gives better results for the monomer cross-linking system, which has the extra contribution of cluster scattering in addition to the frozen concentration fluctuations. This means that the PR theory has a potential misleading static correlator due to the absence of the following consideration: an introduction of cross-links into polymer solutions leads to rather homogeneous structures even if the concentration fluctuations are frozen in the network. Thus, the theory should be improved so as to estimate the proper degree of inhomogeneities for polymer network.

Acknowledgment. This work is supported by Grants-in-Aid Nos. 12450388 and 13750832 and Grant-in-Aid for Scientific Research on Priority Areas (A), "Dynamic Control of Strongly Correlated Soft Materials" (No. 413/13031019) from the Ministry of Education, Science, Sports, Culture, and Technology, Japan. This work was performed with the approval of the Institute for Solid State Physics, The University of Tokyo (Proposal No. 00-0586 and 01-1591), at Japan Atomic Energy Research Institute, Tokai, Japan.

References and Notes

(1) Rossi, D.; Kajiwara, K.; Osada, Y.; Yamauchi, A.; Eds. *Polymer Gels*; Plenum: New York, 1991.
(2) Osada, Y.; Kajiwara, K.; Eds. *Gel Handbook*; Academic Press: New York, 2001.
(3) Hirokawa, Y.; Tanaka, T. *J. Chem. Phys.* **1984**, *81*, 6379.
(4) Tanaka, T. *Sci. Am.* **1981**, *244*, 110.
(5) Shibayama, M.; Tanaka, T. *Adv. Polym. Sci.* **1993**, *109*, 1.
(6) Li, Y.; Tanaka, T. *J. Chem. Phys.* **1989**, *90*, 5161.
(7) Shibayama, M.; Suetoh, Y.; Nomura, S. *Macromolecules* **1996**, *29*, 6966.
(8) Yoshida, R.; Uchida, K.; Kaneko, Y.; Sakai, K.; Kikuchi, A.; Sakurai, Y.; Okano, T. *Nature (London)* **1995**, *374*, 240.
(9) Kabra, B. G.; Gehrke, S. H. *Polym. Commun.* **1991**, *32*, 322.
(10) Kishi, R.; Hirasa, O.; Ichijo, H. *Polym. Gels Networks* **1997**, *5*, 145.
(11) Sayil, C.; Okay, O. *Polym. Bull. (Berlin)* **2002**, *48*, 499−506.
(12) Okajima, T.; Harada, I.; Nishio, K.; Hirotsu, S. *Jpn. J. Appl. Phys.* **2000**, *39*, L875.
(13) Shibayama, M.; Nagai, K. *Macromolecules* **1999**, *32*, 7461.
(14) Naghash, H. J.; Okay, O. *J. Appl. Polym. Sci.* **1996**, *60*, 971.
(15) Patras, G.; Qiao, G. G.; Solomon, D. H. *Macromolecules* **2001**, *34*, 6369.
(16) Ide, N.; Fukuda, T. *Macromolecules* **1999**, *32*, 95.
(17) Shibayama, M.; Norisuye, T.; Nomura, S. *Macromolecules* **1996**, *29*, 8746.
(18) Pusey, P. N.; van Megen, W. *Physica A* **1989**, *157*, 705.
(19) Joosten, J. G. H.; McCarthy, J. L.; Pusey, P. N. *Macromolecules* **1991**, *24*, 6690.
(20) Xue, J. Z.; Pine, D. J.; Milner, S. T.; Wu, X. L.; Chaikin, P. M. *Phys. Rev. A* **1992**, *46*, 6550.
(21) Shibayama, M.; Takeuchi, T.; Nomura, S. *Macromolecules* **1994**, *27*, 5350.
(22) Rodd, A. B.; Dunstan, D. E.; Boger, D. V.; Schmidt, J.; Burchard, W. *Macromolecules* **2001**, *34*, 3339−3352.
(23) Zhao, Y.; Zhang, G.; Wu, C. *Macromolecules* **2001**, *34*, 7404.
(24) Geissler, E. In *Dynamic Light Scattering, the Methods and Applications*; Brown, W., Ed.; Oxford University: Oxford, England, 1993.
(25) Rouf-George, C.; Munch, J.-P.; Schosseler, F.; Pouchelon, A.; Beinert, G.; Boue, F.; Bastide, J. *Macromolecules* **1997**, *30*, 8344.
(26) Panyukov, S.; Rabin, Y. *Phys. Rep.* **1996**, *269*, 1.
(27) Panyukov, S.; Rabin, Y. *Macromolecules* **1996**, *29*, 7960.
(28) Grosberg, A. Y.; Nechaev, S. K. *Macromolecules* **1991**, *24*, 2789.
(29) Kuznetsov, Y. A.; Thimoshenko, E. G.; Dawson, K. A. *J. Chem. Phys.* **1996**, *104*, 3338.
(30) Kuznetsov, Y. A.; Timoshenko, E. G.; Dawson, K. A. *J. Chem. Phys.* **1995**, *103*, 4807.
(31) Norisuye, T.; Masui, N.; Kida, Y.; Shibayama, M.; Ikuta, D.; Kokufuta, E.; Ito, S.; Panyukov, S. *Polymer* **2002**, *43*, 5289−5297.
(32) Takata, S.; Norisuye, T.; Shibayama, M. *Macromolecules* **2002**, *35*, 4779.
(33) Takata, S.; Suzuki, K.; Shibayama, M.; Norisuye, T. *Polymer* **2002**, *43*, 3101.

(34) Sato-Matsuo, E.; Orkisz, M.; Sun, S.-T.; Li, Y.; Tanaka, T. *Macromolecules* **1994**, *27*, 6791.
(35) Shibayama, M.; Takata, S.; Norisuye, T. *Physica A* **1998**, *249*, 245.
(36) de Gennes, P. G. *Scaling Concepts in Polymer Physics*; Cornell University: Ithaca, NY, 1979.
(37) Candau, S. J.; Toung, C. Y.; Tanaka, T.; Lemarechal, P.; Bastide, J. *J. Chem. Phys.* **1979**, *70*, 4694.
(38) Mallam, S.; Horkay, F.; Hecht, A. M.; Geissler, E. *Macromolecules* **1989**, *22*, 3356.
(39) Shibayama, M.; Tanaka, T.; Han, C. C. *J. Chem. Phys.* **1992**, *97*, 6842.
(40) Kubota, K.; Fujishige, S.; Ando, I. *Polym. J.* **1990**, *22*, 15.
(41) Hecht, A. M.; Duplessix, R.; Geissler, E. *Macromolecules* **1985**, *18*, 2167.
(42) Mendes, E.; Girard, B.; Picot, C.; Buzier, M.; Boue, F.; Bastide, J. *Macromolecules* **1993**, *26*, 6873.
(43) Coviello, T.; Burchard, W.; Geissler, E.; Maier, D. *Macromolecules* **1997**, *30*, 2008.

MA030067H